



Dielectric relaxation properties of nanostructured Ce_{0.8}Gd_{0.1}Pr_{0.1}O₂ material at intermediate temperatures

Ashok Kumar Baral and V. Sankaranarayanan

Citation: *Applied Physics Letters* **94**, 074101 (2009); doi: 10.1063/1.3083556

View online: <http://dx.doi.org/10.1063/1.3083556>

View Table of Contents: <http://scitation.aip.org/content/aip/journal/apl/94/7?ver=pdfcov>

Published by the [AIP Publishing](#)

Articles you may be interested in

[Electrical and structural properties of BaCe_{0.90}Y_{0.10}O₃ thin film on MgO \(100\) substrate](#)

J. Appl. Phys. **104**, 113704 (2008); 10.1063/1.3035845

[Grain boundary effects in the granular high-*T_c* superconductor RuSr₂Gd_{1.4}Ce_{0.6}Cu₂O₁₀+](#)

J. Appl. Phys. **103**, 123904 (2008); 10.1063/1.2943270

[Temperature-dependent Raman study of Ce_{0.75}Nd_{0.25}O₂ nanocrystals](#)

Appl. Phys. Lett. **91**, 203118 (2007); 10.1063/1.2815928

[Magnetothermopower and magnetoresistivity of RuSr₂Gd_{2-x}Ce_xCu₂O₁₀ + \(x = 0.6, 1.0\)](#)

Appl. Phys. Lett. **91**, 123110 (2007); 10.1063/1.2784962

[Dopant site selectivity in BaCe_{0.85}M_{0.15}O₃ - by extended x-ray absorption fine structure](#)

J. Appl. Phys. **97**, 054101 (2005); 10.1063/1.1846946

The logo for AIP Chaos is displayed on a red background with a geometric pattern. The letters 'AIP' are in a large, white, sans-serif font, followed by a vertical line and the word 'Chaos' in a smaller, white, sans-serif font.

AIP | Chaos

CALL FOR APPLICANTS
Seeking new Editor-in-Chief

Dielectric relaxation properties of nanostructured $\text{Ce}_{0.8}\text{Gd}_{0.1}\text{Pr}_{0.1}\text{O}_{2-\delta}$ material at intermediate temperatures

Ashok Kumar Baral^{a)} and V. Sankaranarayanan

Department of Physics, Indian Institute of Technology Madras, Chennai 600036, India

(Received 29 November 2008; accepted 27 January 2009; published online 17 February 2009)

The dielectric relaxation behavior of the fluorite structured nanocrystalline $\text{Ce}_{0.8}\text{Gd}_{0.1}\text{Pr}_{0.1}\text{O}_{2-\delta}$ compound was studied in the temperature range of 200–550 °C. Two different types of relaxation processes were observed corresponding to (1) defect pairs such as $(\text{Pr}'_{\text{Ce}}-\text{V}_{\text{O}})^{\bullet}$ and $(\text{Gd}'_{\text{Ce}}-\text{V}_{\text{O}})^{\bullet}$ and (2) the trimers such as $(\text{Pr}'_{\text{Ce}}-\text{V}_{\text{O}}^{\bullet\bullet}-\text{Gd}'_{\text{Ce}})$. The correlation between ionic conduction and the dielectric properties of the nanocrystalline material is discussed. Very low values of the migration energy and association energy of the oxygen vacancies are observed, which are 0.42 and 0.03 eV, respectively. The obtained value of association energy agrees well with the theoretical prediction on doubly doped ceria. © 2009 American Institute of Physics. [DOI: 10.1063/1.3083556]

In recent days, the nanostructured ceria based solid electrolytes have attracted great interest for application in intermediate temperature solid oxide fuel cell. The use of nanocrystalline electrolyte materials has been expected to overcome various drawbacks associated with microcrystalline electrolyte materials such as reduction in Ce^{+4} to Ce^{+3} at higher temperatures¹ and segregation of impurities such as Si or Ca at the grain boundaries.^{2–5} Various nanocrystalline materials of doped and undoped ceria have been synthesized by different methods and studied^{6–10} but their dynamic properties at intermediate temperatures are not yet clear. On the other hand, it has been theoretically predicted that the cerium oxide, doped with double dopants such as Nd/Sm and Pr/Gd whose average atomic numbers lie between 61 and 62, may show high value of ionic conductivity with very low association energy due to a good balance between the elastic and electronic interaction between oxygen vacancies and trivalent ions.¹¹ In the present work, the dielectric relaxation properties of nanostructured $\text{Ce}_{0.8}\text{Gd}_{0.1}\text{Pr}_{0.1}\text{O}_{2-\delta}$ material are studied in the intermediate temperature range to understand the ionic transport mechanism in nanoscale.

The nanocrystalline $\text{Ce}_{0.8}\text{Gd}_{0.1}\text{Pr}_{0.1}\text{O}_{2-\delta}$ material with an average grain size of 14 nm was prepared by citrate auto ignition method.¹² The powder was pressed into a pellet of 10 mm diameter and 1.3 mm thickness. The silver paste was applied on both sides of the pellet for the purpose of electrodes. The dielectric constant ϵ' , loss tangent ($\tan \delta$), and electric modulus M'' were obtained from the electrochemical impedance analysis performed in the ambient conditions in the temperature range of 200–550 °C and in the frequency range of 1 Hz to 10 MHz.

Figure 1 illustrates the high resolution transmission electron microscopy (HRTEM) picture of a $\text{Ce}_{0.8}\text{Gd}_{0.1}\text{Pr}_{0.1}\text{O}_{2-\delta}$ particle from a group of agglomerated particles. It is evident from the micrograph that the microstructure of the nanocrystalline $\text{Ce}_{0.8}\text{Gd}_{0.1}\text{Pr}_{0.1}\text{O}_{2-\delta}$ material consists of arbitrarily oriented well defined single crystalline nanoparticles. The particle size of the material is found to vary between 8 and 18 nm.

From the ac conductivity analysis it is observed that in the temperature range of 200–550 °C, the ionic conduction at both grain interior and grain boundaries contributes to the total conductivity of the material. The total ionic conductivity is found to be dominated by grain interior conductivity at the temperatures of up to 360 °C, whereas at high temperatures the grain boundary conductivity is more than the grain interior conductivity. The activation energy of the material is found to be 1.5 eV below 360 °C and 0.62 eV in the higher temperature region.

The variation in dielectric constant ϵ' with frequency, for the nanocrystalline material, at three different temperatures is shown in Fig. 2. The dielectric constant ϵ' exhibits strong dispersion in the lower frequency region and shows a sharp upturn due to polarization of charge carriers at the electrode-electrolyte interface, as shown in the inset of Fig. 2. In the logarithmic scale, the dielectric constant ϵ' exhibits a step in the low frequency region, as it was observed in $\text{ZrO}_2\text{-Y}_2\text{O}_3$ ceramic solution.¹³ This step could be attributed to the grain boundary relaxation, which leads to the formation of plateau in dielectric constant ϵ' in the low frequency region. With a temperature increase up to 360 °C, the plateau shifts toward lower frequencies and above 360 °C, the

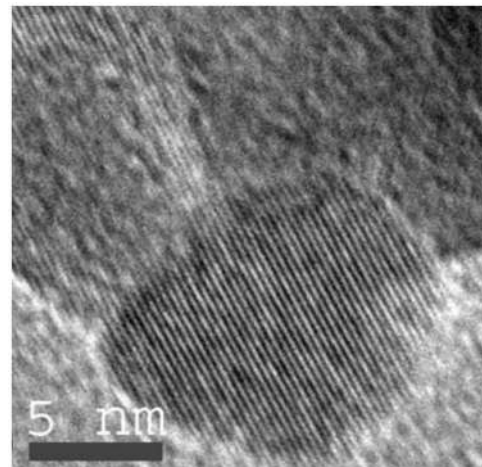


FIG. 1. High resolution TEM micrograph of the nanocrystalline $\text{Ce}_{0.8}\text{Gd}_{0.1}\text{Pr}_{0.1}\text{O}_{2-\delta}$ material calcined at 800 °C. Size of the particle shown here is around 14 nm.

^{a)}Electronic mail: ashok@physics.iitm.ac.in.

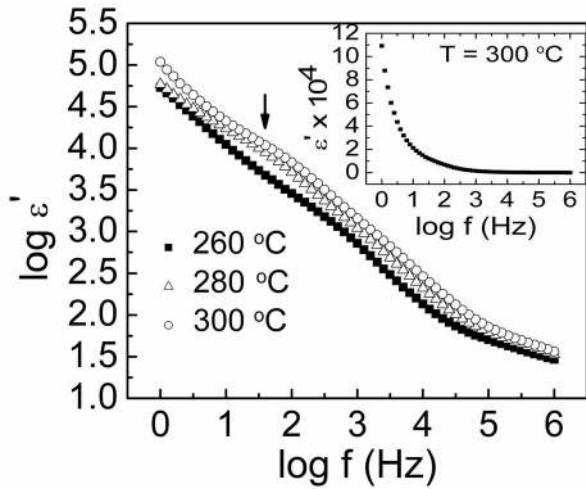


FIG. 2. The variation in $\log \epsilon'$ with frequency at different temperatures. The arrow mark indicates the plateau of grain boundary relaxation. Inset is the variation in ϵ' with frequency at 300 °C.

plateau shifts toward the high frequency region. This behavior of dielectric constant ϵ' in the nanocrystalline material matches well with the ionic conduction mechanism in the temperature range below and above 360 °C as explained above. Hence it implies that the characteristic dielectric relaxation of lattice at the grain boundaries is associated with the migration of charge carriers at grain boundaries in the nanostructured $\text{Ce}_{0.8}\text{Gd}_{0.1}\text{Pr}_{0.1}\text{O}_{2-\delta}$ material. The values of ϵ_∞ (the high frequency limit of ϵ') are found to be 43.52, 41.03, 33.41, and 16.03, respectively, at 380, 400, 460, and 500 °C. The decrease in dielectric constant is found to be associated with the increase in ionic conductivity at higher temperatures.

Figure 3 shows the frequency spectrum of dielectric loss tangent ($\tan \delta$) of the material at 300 °C. The dielectric loss tangent exhibits the presence of two relaxation peaks, which are indicated by arrow marks in the Fig. 3. The high frequency peak could be attributed to the defect pairs formed due to the association of oxygen vacancy with one of the trivalent dopant cations (either Pr^{3+} or Gd^{3+}).^{14,15} In general, when the CeO_2 is doped with trivalent cations, one oxygen

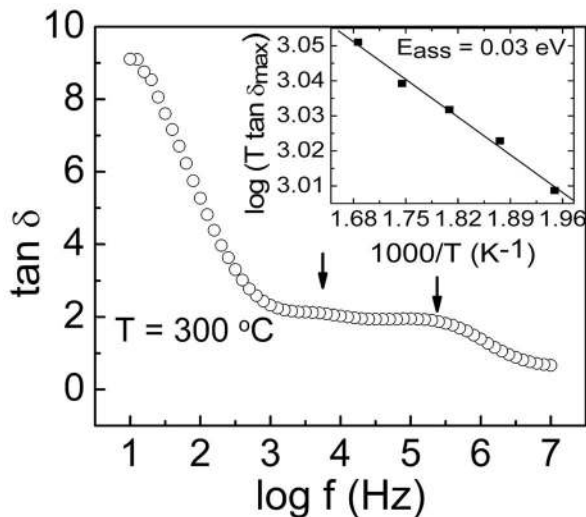
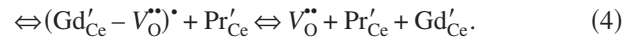
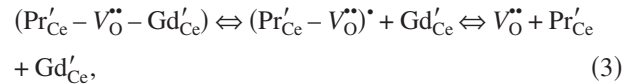
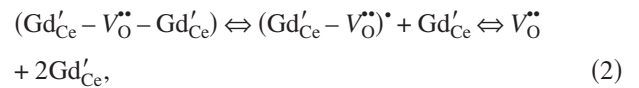
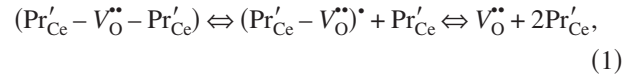


FIG. 3. The frequency spectrum of dielectric loss tangent ($\tan \delta$) at 300 °C. Inset is the Arrhenius plot of $\log(T \tan \delta_{\max})$ vs $1/T$.

vacancy is introduced for every two trivalent ions for the charge neutrality. The trivalent cations replacing Ce^{4+} in the cubic fluorite structure, possess an effective charge of -1 . The mobile oxygen vacancy ($V_{\text{O}}^{\bullet\bullet}$) being positively charged associates with one of the two dopants to make a defect pair, leaving the other one as unassociated defect. Since two types of trivalent cations, i.e., Pr^{3+} and Gd^{3+} , are replacing Ce^{4+} , two different types of defect pairs such as $(\text{Pr}'_{\text{Ce}} - V_{\text{O}})^{\bullet}$ and $(\text{Gd}'_{\text{Ce}} - V_{\text{O}})^{\bullet}$ are expected to be present in the material. Even though these defect pairs are charged, they act like electric dipoles and give rise to dielectric relaxation. The low frequency peak could be ascribed to any of the possible associate neutral trimers¹⁴ such as $(\text{Pr}'_{\text{Ce}} - V_{\text{O}}^{\bullet\bullet} - \text{Gd}'_{\text{Ce}})$, $(\text{Pr}'_{\text{Ce}} - V_{\text{O}}^{\bullet\bullet} - \text{Pr}'_{\text{Ce}})$, or $(\text{Gd}'_{\text{Ce}} - V_{\text{O}}^{\bullet\bullet} - \text{Gd}'_{\text{Ce}})$. The neutral trimer giving rise to the dielectric relaxation peak must be a bended one because the linear trimer cannot show any effective dipole moment and hence there will be no relaxation peak. For the conduction of oxygen ions in this double rare-earth doped ceria nanostructured system, the following equilibrium reactions can be assumed:



In the conduction process, the oxygen vacancies dissociate from the pairs and assist the migration of oxygen ions (O^{2-}). The binding energy (in other words the association energy) " E_{ass} " of the oxygen vacancies can be obtained from the Arrhenius plot of $\log(T \tan \delta_{\max})$ versus $1/T$ (Ref. 14), which is shown as an inset of Fig. 3. Also, the migration energy (E_m) associated with the jump of oxygen vacancies can be obtained from the Arrhenius plot of $\log(f_{\tan \delta})$ versus $1/T$. The association energy (E_{ass}) and the migration energy (E_m) of oxygen vacancies in this nanostructured material are found to be 0.03 and 0.45 eV, respectively.

In the case of nanocrystalline ceria doped with Nd and Sm, Yamamura *et al.*^{15,16} suggested that the plateau or step-like behavior in the variation in dielectric constant ϵ' with frequency can be ascribed to the Debye-type relaxation due to the defect associates. But in the present case, the material shows a single plateau (shown by an arrow mark in the Fig. 2), and the relaxation frequencies estimated from the plateau do not match with those of loss tangent ($\tan \delta$), as those were matching in case of Nd doped ceria.¹⁵ Moreover, the plateau in dielectric constant ϵ' is observed in the entire temperature range, whereas the relaxation peaks in loss tangent ($\tan \delta$) vanish at temperatures above 340 °C. Therefore the plateau observed in frequency dependent plot of ϵ' , in the case of nanostructured $\text{Ce}_{0.8}\text{Gd}_{0.1}\text{Pr}_{0.1}\text{O}_{2-\delta}$ material, could not be ascribed to the relaxation of defect associate. It must be due to dielectric relaxation of grain boundary as already mentioned.

It is observed that both the dielectric constant ϵ' and loss tangent ($\tan \delta$) exhibit strong polarization effect at lower fre-

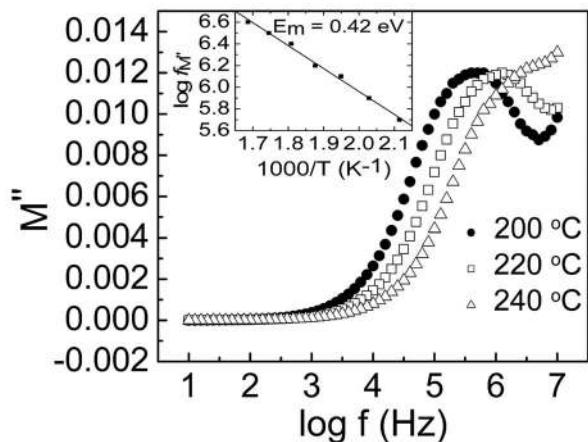


FIG. 4. The frequency spectra of electric modulus M'' at different temperatures. The inset shows the Arrhenius plot of $\log(f_M'')$ vs $1/T$.

quencies. In order to suppress the polarization effect, the dielectric property is explained through electric modulus M'' . Figure 4 shows the frequency spectra of imaginary part of electric modulus M'' at three different temperatures. At lower frequencies the M'' values approach to zero, which indicates that the electrode polarization does not make any significant contribution to the modulus data. At lower temperatures, the modulus spectra exhibit the presence of a relaxation peak. The peak could be attributed to the charge reorientation relaxation of $(\text{Pr}'_{\text{Ce}} - \text{V}_\text{O})^*$ and $(\text{Gd}'_{\text{Ce}} - \text{V}_\text{O})^*$ defect associates in the present system, as observed in microcrystalline La doped ceria by Sarkar and Nicholson.¹⁷ Since oxygen vacancy ($\text{V}_\text{O}^{\bullet\bullet}$) is present in the cubic $\text{Ce}_{0.8}\text{Gd}_{0.1}\text{Pr}_{0.1}\text{O}_{2-\delta}$ material, it can occupy any of the eight equivalent sites, giving rise to a reorientation relaxation process. As the temperature increases, the peak frequency ($f_{M''}$) shifts toward the higher values, showing relaxation nature of the peak. The activation energy for reorientation of oxygen vacancies is obtained from the Arrhenius plot of $\log f_{M''}$ versus $1/T$ (shown as inset of Fig. 4) and is found to be 0.42 eV. The motion of $\text{V}_\text{O}^{\bullet\bullet}$ in this reorientation process is bound motion, i.e., the oxygen vacancy $\text{V}_\text{O}^{\bullet\bullet}$ remains bound to one of the Pr'_{Ce} or Gd'_{Ce} ion and jumps between the nearest neighboring position of these ions in the cubic structure.¹⁷ The jump in bound state motion is similar to that of a free $\text{V}_\text{O}^{\bullet\bullet}$ in the system. Therefore the activation energy for the bound motion is considered as the migration energy of free $\text{V}_\text{O}^{\bullet\bullet}$ in the long range motion.¹⁷ The migration energy (i.e., 0.42 eV) obtained from the modulus spectra matches well with the value obtained from loss tangent ($\tan \delta$). The peak corresponding to the relaxation reorientation of defect pairs is found to vanish completely at temperatures above 360 °C. So it indicates the existence of local motion of oxygen vacancies in the nanostructured $\text{Ce}_{0.8}\text{Gd}_{0.1}\text{Pr}_{0.1}\text{O}_{2-\delta}$ material at lower temperatures, and at temperatures above 360 °C, the oxygen vacancies are completely free for long range migration. Generally it is expected that the concentration of free oxygen vacancy is higher at grain boundaries in high temperature region. Since the oxygen vacancies are found to be completely free above 360 °C, these results in the increase in grain boundary contribution to the total conductivity and the reduction in total activation energy of the material. Therefore the grain boundary conductivity dominates the whole conduction process at the tem-

peratures above 360 °C as mentioned earlier.

The values of migration energy ($E_m=0.42$ eV) and association energy ($E_{\text{ass}}=0.03$ eV) of oxygen vacancies in the nanostructured $\text{Ce}_{0.8}\text{Gd}_{0.1}\text{Pr}_{0.1}\text{O}_{2-\delta}$ material are found to be very low compared to the experimentally observed values in various microcrystalline electrolyte materials.^{18,19} Also, the association energy (E_{ass}) of oxygen vacancies in this material is almost close to the lowest theoretical value, 0.02 eV for Pm^{+3} doped ceria.¹¹ The reason for low value of association energy could be due to the optimum balance between the elastic and electronic interactions of oxygen vacancies with the trivalent dopants Gd'_{Ce} and Pr'_{Ce} . Hence the experimental result on nanocrystalline $\text{Ce}_{0.8}\text{Gd}_{0.1}\text{Pr}_{0.1}\text{O}_{2-\delta}$ material is found to agree well with the recent theoretical prediction¹¹ that the double doped ceria with possible combination Pr/Gd, whose average atomic numbers lie between 61 and 62, may show very low association energy between the oxygen vacancies and trivalent dopant ions.

In summary, the dielectric relaxation of lattice at the grain boundaries is found to be associated with the motion of charge carriers at the grain boundaries. Two types of dielectric relaxation processes corresponding to defects pairs and trimers are observed, which are associated with the motion of oxygen vacancies in the nanocrystalline $\text{Ce}_{0.8}\text{Gd}_{0.1}\text{Pr}_{0.1}\text{O}_{2-\delta}$ material at lower temperatures. The observed low value of association energy leads to the increase in grain boundary conductivity, as well as reduction in total activation energy at the temperatures above 360 °C. The migration energy and the association energy of oxygen vacancies in this material are found to be very low compared to those in various microcrystalline materials. Also, the observed value of association energy is found to agree well with the theoretical concept on association energy in the ceria doped with two trivalent cations.

¹M. Mogensen, N. M. Sammes, and G. Tompsett, *Solid State Ionics* **129**, 63 (2000).

²R. Gerhardt and A. S. Nowick, *J. Am. Ceram. Soc.* **69**, 641 (1986).

³R. Gerhardt, A. S. Nowick, M. E. Mochel, and I. Dumler, *J. Am. Ceram. Soc.* **69**, 647 (1986).

⁴D. Y. Wang and A. S. Nowick, *J. Solid State Chem.* **35**, 325 (1980).

⁵M. J. Verkerk, B. J. Middelhuis, and A. J. Burggraaf, *Solid State Ionics* **6**, 159 (1982).

⁶A. Hartridge, A. K. Bhattacharya, R. E. Dunin-Borkowski, and J. L. Hutchison, *J. Nanopart. Res.* **3**, 431 (2001).

⁷J. M. Im, H. J. You, Y. S. Yoon, and D. W. Shin, *J. Eur. Ceram. Soc.* **27**, 3671 (2007).

⁸E. Rossinyol, E. Pellicer, A. Prim, S. Estrade, J. Arbiol, F. Peiro, A. Cornet, and J. R. Morante, *J. Nanopart. Res.* **10**, 369 (2008).

⁹X. Sha, Z. Lu, X. Huang, J. Miao, Z. Ding, X. Xin, and W. Su, *J. Alloys Compd.* **428**, 59 (2007).

¹⁰T. Mori, T. Kobayashi, Y. Wang, J. Drennan, T. Nishimura, J. Li, and H. Kobayashi, *J. Am. Ceram. Soc.* **88**, 1981 (2005).

¹¹K. Muthukkumar and R. Bokalawela, *J. Mater. Sci.* **42**, 7461 (2007).

¹²A. K. Baral and V. Sankaranarayanan, Proceedings of International INCCOM-6 Conference on Future Trend in Composite Materials and Processing, 2007 (unpublished).

¹³A. Pimenov, J. Ullrich, P. Lunkenheimer, A. Loidl, and C. H. Ruscher, *Solid State Ionics* **109**, 111 (1998).

¹⁴M. Kurumada, H. Hara, and E. Iguchi, *Acta Mater.* **53**, 4839 (2005).

¹⁵H. Yamamura, S. Takeda, and K. Kakinuma, *Solid State Ionics* **178**, 1059 (2007).

¹⁶H. Yamamura, S. Takeda, and K. Kakinuma, *Solid State Ionics* **178**, 889 (2007).

¹⁷P. Sarkar and P. S. Nicholson, *J. Am. Ceram. Soc.* **72**, 1447 (1989).

¹⁸R. Gerhardt-Anderson and A. S. Nowick, *Solid State Ionics* **5**, 547 (1981).

¹⁹J. A. Kilner, *Solid State Ionics* **8**, 201 (1983).